



Supplementary Information for

**Astroglial FMRP Deficiency Cell-autonomously Upregulates miR-128 and Disrupts
Developmental Astroglial mGluR5 Signaling**

Yuqin Men¹, Liang Ye^{3,4}, Ryan Risgaard^{5,6}, Vanessa Promes¹, Xinyu Zhao^{5,6},
Martin Paukert^{3,4}, Yongjie Yang^{1,2*}

¹Tufts University, Department of Neuroscience, 136 Harrison Ave, Boston, MA, 02111

²Tufts University, Graduate School of Biomedical Sciences, 145 Harrison Ave, Boston, MA, 02111

³University of Texas Health Science Center at San Antonio, Department of Cellular and Integrative Physiology, 8403 Floyd Curl Drive, STRF 208.2, San Antonio, TX, 78229

⁴Center for Biomedical Neuroscience, University of Texas Health Science Center at San Antonio, San Antonio, TX, 78229

⁵Waisman Center, University of Wisconsin-Madison, Madison, WI, 53705

⁶Department of Neuroscience, University of Wisconsin-Madison, Madison, WI, 53705

*Corresponding author: Yongjie Yang, Tufts University, Department of Neuroscience, 136 Harrison Ave, Boston, MA 02111. Phone: 617-636-3643; Fax: 617-636-2413; Email: yongjie.yang@tufts.edu; ORCID: 0000-0003-0318-8224

Includes:

Figs. S1 to S7

Legend for Figs. S1 to S7

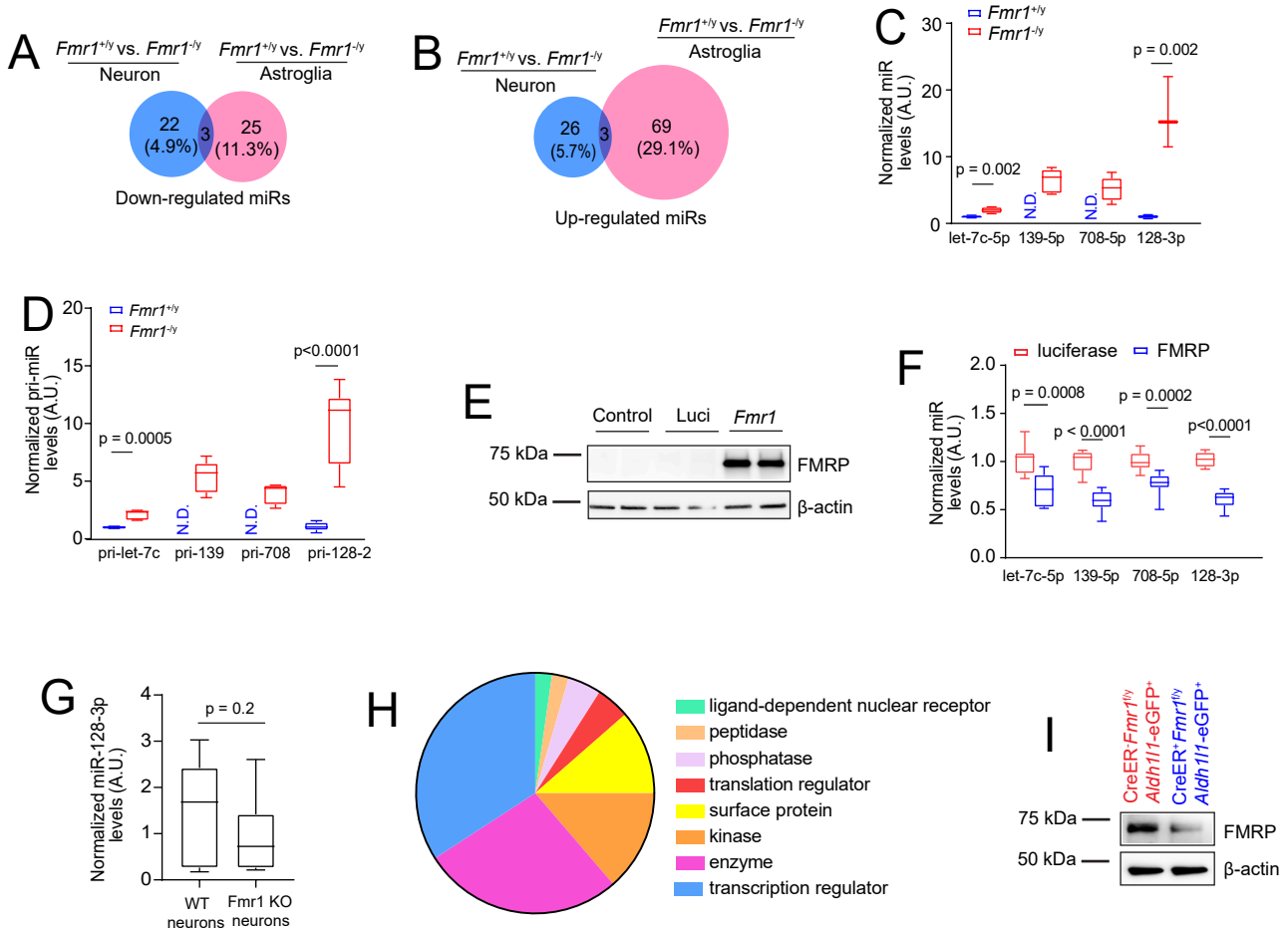


Figure. S1

Fig. S1 FMRP preferentially suppress miR biogenesis in astroglia

Venn diagram of the down- (A) and up-regulated (B) miRs in cultured *Fmr1*^{+/-} and *Fmr1*^{-/-} astroglia and neurons. Differentially expressed miRs were identified by miR microarray hybridization. n=3 biologically independent samples per condition. miRs with expression values < 2³ arbitrary unit (A.U.) from the microarray hybridization were deemed not expressed. Percentage in the Venn diagram was calculated by up- or down-regulated miRs divided by total number of detectable miRs in astroglia or neurons; C, Relative expression levels of representative miRs in *Fmr1*^{+/-} and *Fmr1*^{-/-} astroglia by qPCR. All original Ct values are within 26-33 range; N.D.; not detected (Ct ≥ 35). U6 small nuclear (sn) RNA was used as the endogenous control; n = 5 biologically independent samples per condition. D, Relative expression levels of primary miR transcript (pri-miR) of representative miRs in *Fmr1*^{+/-} and *Fmr1*^{-/-} astroglia by qPCR. All original Ct values are within 28-34 range; N.D.: not detected (Ct ≥ 35). β-actin mRNA was used as the endogenous control; n= 5 biologically independent samples per condition. E, Representative immunoblot of FMRP re-expression following *Fmr1* cDNA transfection in cultured *Fmr1*^{-/-} astroglia. F, Relative expression levels of representative miRs in FMRP re-expressed *Fmr1*^{-/-} astroglia by qPCR. All original Ct values are within 22-32 range. U6 RNA was used as the endogenous control. n= 6 biologically independent samples per condition. G, Expression levels of miR-128-3p in *Fmr1*^{+/-} and *Fmr1*^{-/-} astroglia primary neurons by qPCR. n = 9 independent neuronal cultures. p values were determined using two-tailed unpaired t-test. H, Pie chart showing functional categories of genes that are expressed in human and mouse astroglia and are also predicted miR-128-3p binding targets. TargetScan was used to identify putative miR-128-3p target mRNAs. Ingenuity pathway analysis was used for characterizing functional categories. Only genes that are expressed in both human and mouse astroglia (FPKM > 10 and the miR-128-3p-binding

site was conserved in both mouse and human) were included in generating the pie chart. **I**, Representative immunoblot of FMRP in acutely sorted cortical astroglia from 4-OHT-injected astroglial cKO (*Slc1a3*-CreER⁺*Fmr1*^{f/y}*Aldh1l1*-eGFP⁺) mice at P14. p values were determined using two-tailed unpaired t-test. For **C**, **D**, and **F**, the data was presented in the box and whisker plot with defined elements, median (center line), upper and lower quartiles (bounds of box), and highest and lowest values (whiskers).

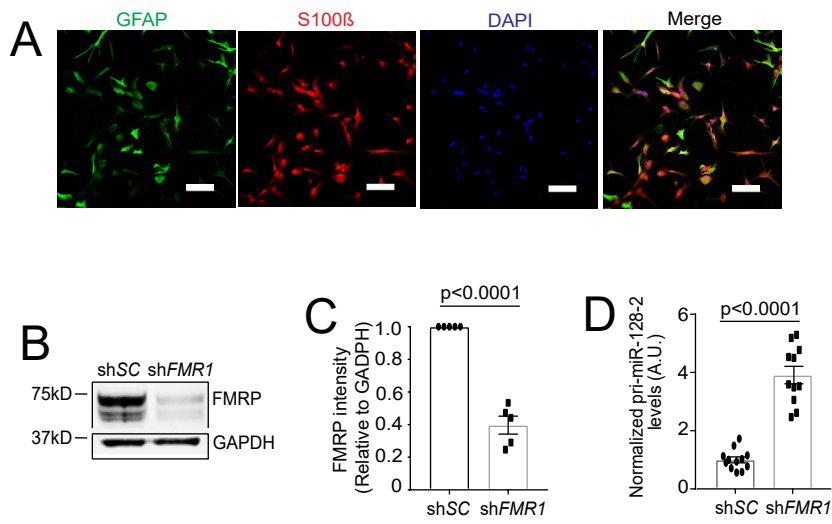


Figure. S2

Fig. S2 FMRP knockdown promotes miR-128 transcription in human astroglia

A, Representative immunostaining images of glial markers GFAP and S100 β in H1 astroglia (7-days post-differentiation) following 7-month astroglial progenitor cell (APC) culture. Scale bar: 100 μm . Representative immunoblot (**B**) and quantification (**C**) of FMRP following lentiviral shRNA-mediated knockdown of FMRP in H1 astroglia. Data are mean \pm SEM of n = 5 biologically independent samples/group with Welch's t-test. **D**, Quantification of pri-miR-128-2 levels by qPCR in lentiviral sh-*scrambled control* (shSC) and sh*FMR1* infected H1 astroglia. Data are mean \pm SEM of n = 11-12 wells/group with Mann-Whitney U test.

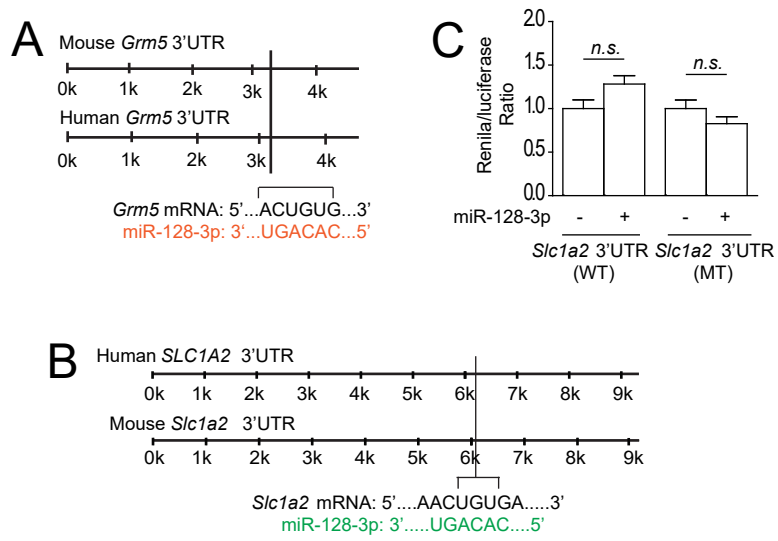


Figure. S3

Fig. S3 Bioinformatic analysis of predicted miR-128-3p target mRNAs that are expressed in astroglia

Bioinformatic analysis of the conserved miR-128-3p binding site on human and mouse *Grm5* (A) or *Slc1a2* (B) mRNA 3'-UTR sequence. C, Wild-type (WT) and miR-128-3p mutant (MT) *Slc1a2* 3' UTR luciferase activity in HEK 293 cells following miR-128-3p transfection. n = 3 independent experiments with six replicates per experiment per condition; p value was determined using two-tailed unpaired t-test.

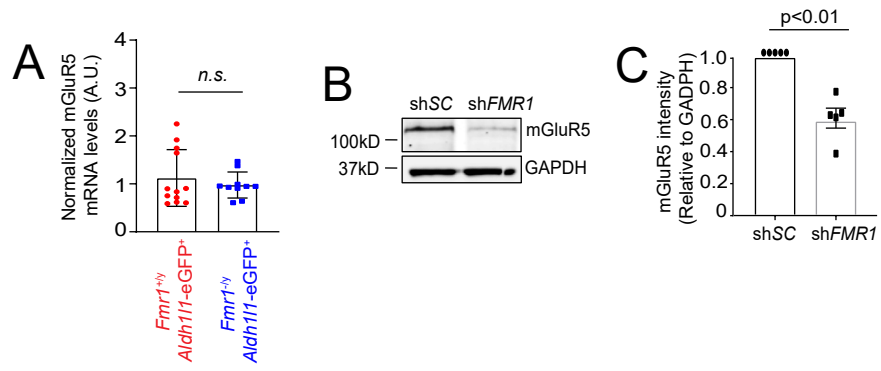


Figure. S4

Fig. S4 Loss of astroglial *Fmr1* down-regulates mGluR5 protein but not mRNA expression

A, Expression levels of mGluR5 mRNA in FAC sorted cortical astroglia from *Fmr1*^{+/*y*}*Aldh111*-eGFP⁺ and *Fmr1*^{-/*y*}*Aldh111*-eGFP⁺ mice at P14; n=5-6 biologically independent samples per condition. p value was determined using two-tailed unpaired t-test. Representative immunoblot (**B**) and quantification (**C**) of mGluR5 protein following lentiviral shRNA-mediated knockdown of FMRP in H1 astroglia. Data are mean ± SEM of n = 5 biologically independent samples/group with Welch's t-test test.

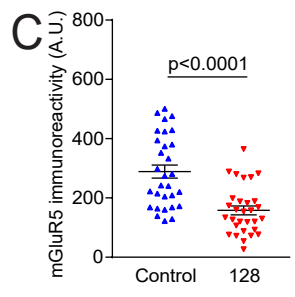
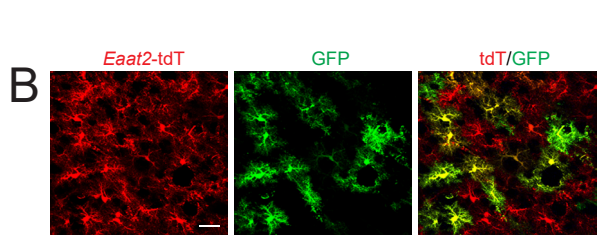
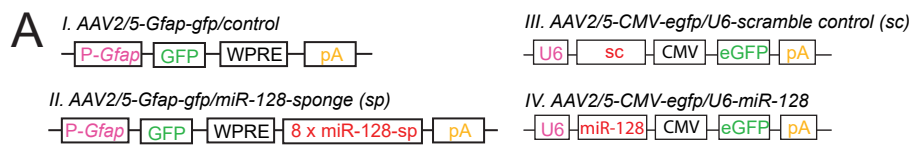


Figure. S5

Fig. S5 Developmental expression of astroglial mGluR5 is cell-autonomously regulated by miR-128-3p *in vivo*

A, Diagram of AAV constructs for gain- and loss-of-function analysis of miR-128-3p *in vivo*. Subpanels: AAV2/5-*Gfap*-GFP/miR-128-control (I), AAV5-*Gfap*-GFP/miR-128-sponge (II), AAV2/5-*CMV*-GFP/U6-scramble control (III), and AAV2/5-*CMV*-GFP/U6-miR-128 (IV). **B**, Representative images of GFP-miR-128-sp expression in cortex of *Fmr1*^{-y}*Eaat2*-tdT⁺ mice. Scale bar: 30 μm. **C**, Quantification of mGluR5 immunoreactivity within individual astroglial domains after miR-128-3p overexpression in *Fmr1*^{+y}*Eaat2*-tdT⁺ mice n = 30–45 cells/4 mice per group; p values were determined using two-tailed unpaired t-test.

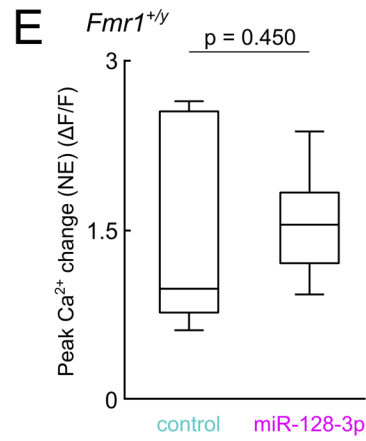
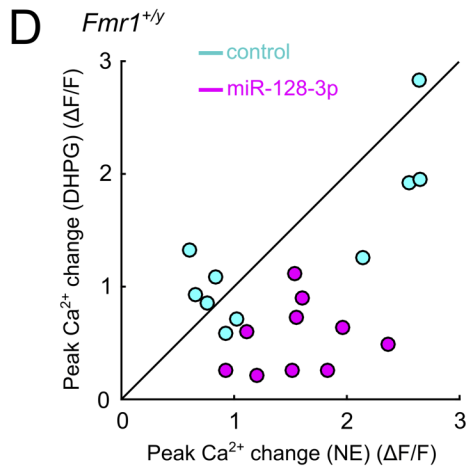
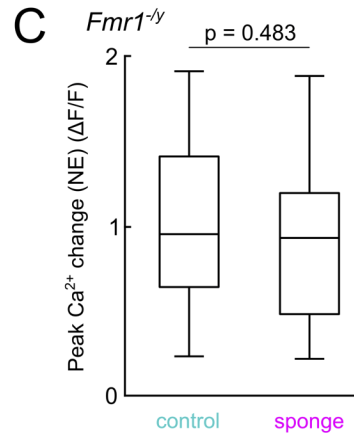
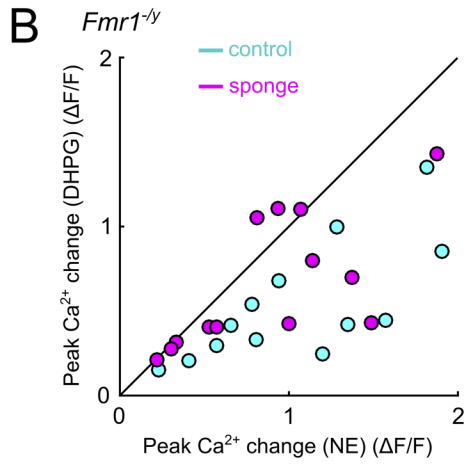
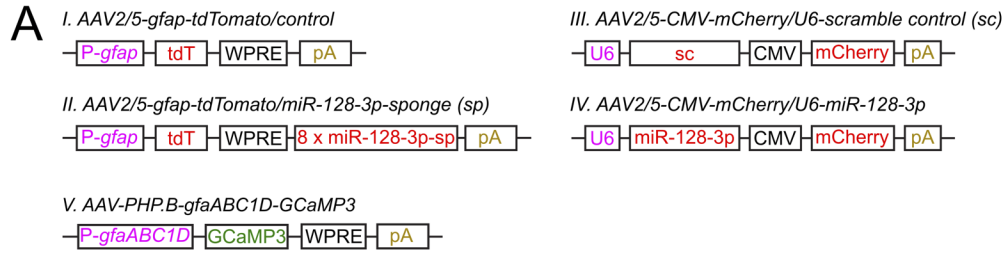


Figure. S6

Fig. S6 *In vivo* expression of miR-128-3p cell-autonomously regulate developmental astroglial mGluR5 signaling

A, Diagram of viral constructs used in two-photon Ca^{2+} imaging. Subpanels: I: AAV2/5-*Gfap*-tdTomato/control; II. AAV2/5-*Gfap*-tdTomato/miR-128-sponge; III. AAV2/5-*CMV*-mCherry/U6-scramble control; IV. AAV2/5-*CMV*-mCherry/U6-miR-128; V. AAV-PHP.B-gfaABC1D-GCaMP3; **B**, Scatter plot comparing averaged Ca^{2+} changes in astroglia from individual slice in response to either DHPG or NE in control or sponge AAV injected *Fmr1*^{-y} mice, respectively. Cyan color filled circle: scrambled control; Magenta color filled circle: miR-128-3p sponge. Diagonal line: identical responses to DHPG and NE; **C**, Boxplot of astroglial peak Ca^{2+} response in *Fmr1*^{-y} slice induced by NE following control (median: 0.942; minimum to maximum: 0.230 to 1.906) or sponge (median: 0.936; minimum to maximum: 0.221 to 1.875) AAV injections; p values were calculated from the Student's t-test. **D**, Scatter plot comparing averaged Ca^{2+} changes in astroglia from individual slice in response to either DHPG or NE in control of miR-128 AAV injected *Fmr1*^{+y} mice, respectively. Cyan color filled circle: scrambled control; Magenta color filled circle: miR-128. **E**, Boxplot of astroglial peak Ca^{2+} response in *Fmr1*^{+y} slice induced by NE following control (median: 0.975; minimum to maximum: 0.608 to 2.646) or miR-128 (median: 1.545; minimum to maximum: 0.929 to 2.368) AAV injection; p values were calculated from the Student's t-test. For **C** and **E**, the data was presented in the box and whisker plot with defined elements, median (center line), upper and lower quartiles (bounds of box), and highest and lowest values (whiskers).

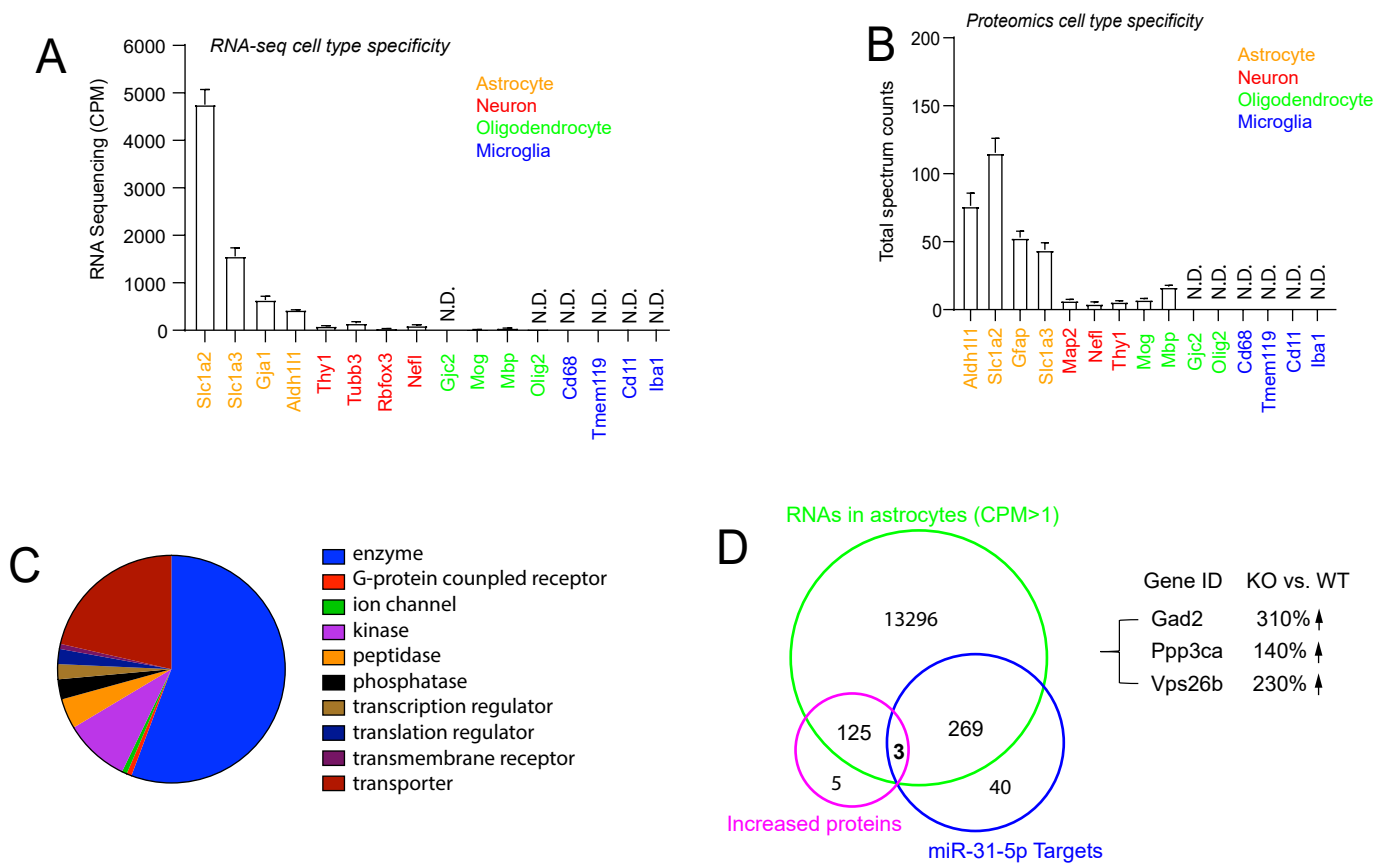


Figure. S7

Fig. S7 Genome-wide transcriptome and proteomics analysis of *Fmr1*^{+/-} and *Fmr1*^{-/-} astroglia

A, Expression levels (CPM) of representative cell type specific gene markers for astroglia, neurons, oligodendrocytes, and microglia in TRAP/RNA-seq data from *Fmr1*^{+/-}*Aldh1l1*-TRAP and *Fmr1*^{-/-}*Aldh1l1*-TRAP mice. n=3 biologically independent samples per condition. N.D.: not detectable; **B**, Expression levels (total spectral counts) of representative cell type specific protein markers for astroglia, neurons, oligodendrocytes, and microglia in LC-MS/MS proteomics data. n=3 biologically independent samples per condition. **C**, Pie chart showing functional categories of DEPs between *Fmr1*^{+/-} and *Fmr1*^{-/-} astroglia using Ingenuity pathway analysis. **D**, Identification of up-regulated proteins in *Fmr1*^{-/-} astroglia whose mRNAs have predicted miR-31-5p binding sites. Venn diagram showing the number of expressed mRNAs (CPM>1) and up-regulated proteins, as well as predicted miR-31-5p mRNA targets, respectively. There are 3 mRNAs having miR-31-5p binding targets and also encoding for proteins that are up-regulated in *Fmr1*^{-/-} astroglia compared to in *Fmr1*^{+/-} astroglia. These 3 genes and their protein expression changes in *Fmr1*^{-/-} vs. *Fmr1*^{+/-} astroglia were shown.